DISPERSIVE WAVES PROPAGATING ALONG A SURFACE FRACTURE

BRADLEY C. ABELL[*] AND LAURA J. PYRAK-NOLTE[†]

Abstract. Significant work in the past few decades has lead to a well developed understanding of seismic wave propagation in fractured media. However, previous research has focused on fractures within rock as opposed to fractures at the surface of a rock. A theoretical and experimental study was performed to examine seismic wave propagation along a fracture at the surface, i.e., along the intersection of two quarter-spaces. A theoretical model that couples two wedges, using displacement discontinuity boundary conditions, was developed that gives rise to a new guided waveform that is dispersive, depends on fracture specific stiffness at the intersection of a fracture with a free surface and exhibits velocities that range from the single wedge-mode velocity to the Rayleigh wave velocity at a free surface. The existence and behavior of this new guided-mode was verified using a synthetic fracture created between two aluminum blocks. This new guided-mode enables characterization of fracture specific stiffness of fractures, joints and other discontinuities at the surface of an outcrop.

1. Introduction. Seismic exploration most commonly uses body waves such as compressional and shear waves to interrogate the subsurface, delineate structure and to monitor physical processes. Other methods also include using the dispersion of surface waves (e.g. Rayleigh, Love), to delineate near and subsurface features [1-3]. For near surface characterization, it is important to understand the effect of fractures on surface wave propagation. Previously, researchers have shown that generalized coupled-Rayleigh waves (i.e., fracture interface waves) propagate along single fractures [4-12]. Theoretically, the fracture is represented as a non-welded interface [13] (i.e. continuous stress but a discontinuity in displacement across the interface) between two elastic half-spaces. Fracture interface waves travel with speeds that depend on the frequency of the signal and stiffness of the fracture. For low fracture specific stiffness (i.e., few areas of contact) the interface wave travels at the Rayleigh wave velocity because the fracture behaves similar to a free surface [5]. When a fracture is closed and the specific stiffness is high, then the interface wave travels as a bulk shear wave, i.e. the interface behaves as a welded contact.

Abell et al. (2012) [14] performed experiments to determine if fracture interface waves exist along the intersection between two orthogonal fractures. From their work, they observed interface-wave like modes that traveled between the Rayleigh wave and bulk shear wave velocities as the stress on the intersection increased, thereby increasing the stiffness. However, at low applied stress, they observed a mode traveling with speeds slower than the Rayleigh wave, a region not possible for interface waves. Wedge-waves are a type of guided mode that travels with velocities lower than the Rayleigh wave velocity [15-17]. A wedge-wave travels along the corner formed when two planes intersect. This wedge wave can exist for a large range of wedge angles. Recently, Sokolova et al. (2012) showed the existence of a new type of waveform, known as a Rayleigh-Stoneley (RS) wave that travels at the surface of two quarter-spaces along a welded contact at the interface between two dissimilar media [18] and with speed slower than the Rayleigh wave. Although theoretically interesting, their analysis has little application to geophysics because of the small range of existence for this wave and the need for materials with density and moduli ratios that range between 0.10 and 0.35. This Rayleigh-Stoneley mode does not exist when the material properties on either side of the interface are the same (like for a fracture in rock).

In this paper, we demonstrate, theoretically and experimentally, that a new-mode, a Rayleigh-Wedge wave (RW), exists along a fracture (i.e., non-welded contact) between two quarter-spaces (Figure 1) with identical density and moduli. This RW mode propagates at the surface along the edge formed by two elastic quarter spaces in partial contact. To the best of the authors' knowledge, this is the first time this mode has been quantified, theoretically and experimentally, and used to estimate the near-surface stiffness of a fracture.

───────

[*]Physics Department, Purdue University, West Lafayette, IN (babell@purdue.edu)

[†]Physics Department, School of Civil Engineering, and the Department of Earth and Atmospheric Sciences, Purdue University, West Lafayette, IN
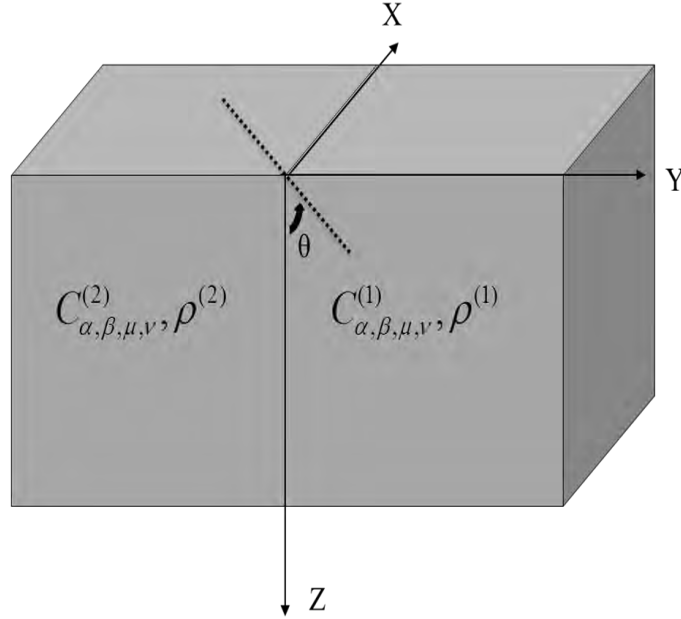
FIG. 1. *Geometry of the problem for coupling wedge waves. A wave propagates along the x-axis. C represents the elastic constants and is the density of each medium. The angle, θ, is used for reference to the transducer polarization. The superscripts 1 and 2 refer to the two media that can have similar or dissimilar material properties.*

2. Theory. Our theoretical formulation for the RW mode is based on coupled wedge waves. Wedge waves were originally postulated for use as waveguides [15] and phonon propagation in crystals [16], yet their applications have found many areas of use [19]. More recently theoretical work has begun to couple these waveforms with continuous boundary conditions [18, 20]. Although theoretically intriguing, these RS waveforms were found to exist only for two different media in contact, with a small range of physical parameters that are unlikely to be useful or found in the field. Our theory is based on the work originally done by Sokolova et al (2012) [18] for a welded contact and so a brief outline of their work will be presented with more emphasis on the new results from displacement discontinuity boundary conditions.

2.1. Problem Geometry. The theoretical formulation for RW modes is applicable for two quarter spaces, medium 1 and 2, in contact (Figure 1). Medium 1 exists in the region $x > 0, y > 0, z > 0$ with density $\rho(1)$ and elastic constants $C(1)$ and medium 2 occupies the region $x > 0, y < 0, z > 0$ with density $\rho(2)$ and elastic constants $C(2)$. These form a free surface along the $x - y$ plane at $z = 0$, and a fracture plane intersecting this free surface at $y = 0$ along the $x - z$ plane (Figure 1). In the theory that follows the final superscript will represent a medium.

2.2. Boundary Conditions. Unlike the RS modes of Sokolova et al. (2012) mentioned above, this work will use continuity of stress and displacement discontinuity boundary conditions [13, 21], leading to velocity dispersion that depends on fracture specific stiffness and frequency. The displacement and stress amplitude and T respectively, have boundary conditions given by:

$$(2.1) \qquad \tilde{U}_\alpha^{(1)} - \tilde{U}_\alpha^{(2)} = \frac{\tilde{T}_{\alpha,y}^{(1)}}{\kappa_\alpha}, \alpha = x, y, z$$

$$(2.2) \qquad \tilde{T}_\alpha^{(1)} = \tilde{T}_\alpha^{(2)}, \alpha = x, y, z$$

where κ_α is the stiffness along the α direction.

2.3. Theoretical Formulation. If we define the displacement and stress field as

$$(2.3) \qquad u_\alpha(x,y,z;t) = \mathrm{e}^{\mathrm{i}(kx-wt)}\tilde{U}_\alpha(y,z|k) + \mathrm{e}^{-\mathrm{i}(kx-wt)}\tilde{U}_\alpha^*(y,z|k)$$

$$(2.4) \qquad T_{\alpha,\beta}(x,y,z;t) = \mathrm{e}^{\mathrm{i}(kx-wt)}\tilde{T}_{\alpha,\beta}(y,z|k) + \mathrm{e}^{-\mathrm{i}(kx-wt)}\tilde{T}_{\alpha,\beta}^*(y,z|k)$$

where ω is angular frequency, t is time, * is the complex conjugate, and k is the wave number ($k = \frac{\omega}{v}$). Equations (3) & (4) are substituted into the equation of motion and rearranged such that,

$$(2.5) \qquad -\rho\omega^2\tilde{U}_\alpha = \sum_{\beta,\mu,\nu=1}^{3} D_\beta(k)C_{\alpha,\beta,\mu,\nu}D_\nu(k)\tilde{U}_\alpha$$

where the operators D are defined by

$$(2.6) \qquad D_1(k) = \mathrm{i}k, \ \ D_2(k) = \frac{\partial}{\partial \mathrm{y}}, \ \ D_3(k) = \frac{\partial}{\partial \mathrm{z}}$$

Representing the displacement field as a linear sum of Laguerre functions, originally used by Maradudin et al. [16], a relationship between the expansion coefficients and the stress amplitudes are derived [18] and related by the matrix M, given by Equation 11 in Sokolova.

The formulation is identical to Sokolova et al (2012) from Equation 11 through Equation 13. At this point, we apply the displacement discontinuity boundary conditions (1) and (2) above, using the definition of G from Sokolova, to obtain:

$$(2.7) \qquad \frac{1}{k}\left[U_n^{(\alpha,1)} - U_n^{(\alpha,2)}\right] = \frac{1}{\kappa_\alpha}\tau_n^{(\alpha,1)}$$

$$(2.8) \qquad -\bar{G}^{-1\ (\alpha,\beta,1)}\bar{U}_n^{(\alpha,1)} = \bar{G}^{-1\ (\alpha,\beta,2)}\bar{U}_n^{(\alpha,2)}$$

which are used together to obtain,

$$(2.9) \qquad \left[-\bar{G}^{-1\ (\alpha,\beta,1)}\bar{G}^{-1\ (\alpha,\beta,2)}\frac{k}{\kappa_\alpha} - \bar{G}^{-1\ (\alpha,\beta,1)} - \bar{G}^{-1\ (\alpha,\beta,2)}\right]\bar{U}_n^{(\alpha,2)} = 0$$

which can be represented as an eigenvalue problem. This has has solutions when

$$(2.10) \qquad det[\bar{G}^{-1\ (\alpha,\beta,1)}\bar{G}^{-1\ (\alpha,\beta,2)}\frac{k}{\kappa_\alpha} + \bar{G}^{-1\ (\alpha,\beta,1)} + \bar{G}^{-1\ (\alpha,\beta,2)}] = 0$$

We used Equation 10 to determine the range of existence and the velocity of the RW mode for a fracture edge.

2.4. Stiffness Conditions. The fracture specific stiffness in Equation 10 has components in both the normal and tangential directions [13]. For the remainder of this paper, isotropic media will be assumed and both media will be set to the same physical parameters ($C(1) = C(2)$), a case not possible for RS waves [18].

Because of the isotropic nature of this particular study, it was assumed that the shear stiffness along the z-direction was 0 (Figure 1). This was assumed because the wave must decay quickly in the z-direction. Although studies have found that normal to shear stiffness ratios should be on the order of 0.5 for solid-solid boundaries [22, 23], Choi et al (2013) has recently shown that the ratio of normal to shear stiffness depends on how well mated the fracture planes are, fracture roughness and loading conditions (uni-axial vs. bi-axial) [24]. For a first order approximation, a ratio of one was used for the normal to shear stiffness.

2.5. Numerical Simulations. Numerical trials were performed to determine the solution to Equation 10 using the physical parameters listed in Table 2.1 for orders up to $n = m = 15$. The parameters listed were experimentally measured for aluminum samples to compare to our experimental results.

TABLE 2.1
Physical parameters measured for the aluminum samples. These values were used in the numerical analysis section to calculate the velocity.

Numerical Parameters	
$\rho^{(1/2)}$	$2700 \frac{kg}{m^3}$
Lame's Constant μ	$2.55 \times 10^{10} \ Pa$
Lame's Constant λ	$5.25 \times 10^{10} \ Pa$
Shear Velocity	$3075 \ \pm \ 2.5 \frac{m}{s}$
Rayleigh Velocity	$2879 \ \pm \ 2.5 \frac{m}{s}$
Wedge Velocity	$2812 \ \pm \ 2.5 \frac{m}{s}$
Compressional Velocity	$6192 \ \pm \ 2.5 \frac{m}{s}$
Angular Frequency, ω	$2\pi(0.4 MHz)$

Rayleigh-Wedge mode velocities were found for (1) constant frequency with varying stiffness and (2) constant stiffness with varying frequency. From our analysis, the RW mode ranges in velocity from the wedge velocity to the Rayleigh velocity (Figure 2). This is in agreement with the limits of Equation 10. As $\kappa \to \infty$, the first term in Equation 10 $\to 0$ resulting in the same solution for the RS wave, which for the same parameters is just a Rayleigh wave. In a similar manner, as $\kappa \to 0$, the media become decoupled, and each wedge is essentially coupled to vacuum leaving only a wedge wave, i.e. Equation 10 becomes $det[G(1)] = 0$, which is the solution put forth by Maradudin et al. [16].

The dispersion curves collapse to a single curve when the velocity is normalized by the Rayleigh velocity, and the stiffness is normalized by the frequency times the seismic impedance ($Z = \rho v_{shear}$) where v_{shear} is the shear velocity. The result is the single curve, shown in Figure 2 that can be used to estimate the stiffness of the fracture at the surface of a rock or sample if the velocity, frequency and matrix material properties are known.

2.6. Experimental. To verify the existence of this theoretically-derived guided mode, a experiments were performed on aluminum blocks measuring 0.3 m x 0.3 m x 0.3 m to measure the Rayleigh-Wedge mode as a function of stress. The aluminum blocks were machined smooth such that there was no visible roughness on the sample faces. Large blocks were used because the Rayleigh and Wedge wave velocity travel within 7% of each other, making it difficult to separate the waveforms observed for small samples.

Two aluminum blocks were stacked, vertically but rotated by 90°, to form the geometry shown in Figure 1. The blocks were placed in a single axis Instron 100 klbs load frame to apply a load normal to the fracture plane (Figure 3). An Instron Model 59-R8100BTE controller, using Bluehill3 software monitored and applied the desired load to the sample. The sample was loaded from 0 kN to 400.3 kN in steps of 2.22 kN. Once the desired load was reached, the load was maintained while seismic waveforms were propagated at the surface of the blocks along the fracture ($y = 0$ and $z = 0$ in Figure 1).

Seismic transducers, with a central frequency of 1 MHz (Olympus Panametrics V103 and V153) were used to propagate compressional (P) waves and shear (S) waves along the fracture. The transducers were coupled to the samples using honey and a frame was used to attach the transducers to the sample (Figure 3).

Signals were recorded for waves propagated along the surface, along the fracture at the surface of the block, along the fracture deeper in the block and through the bulk material at each applied load. These measurements were done using different transducers such that each location could be
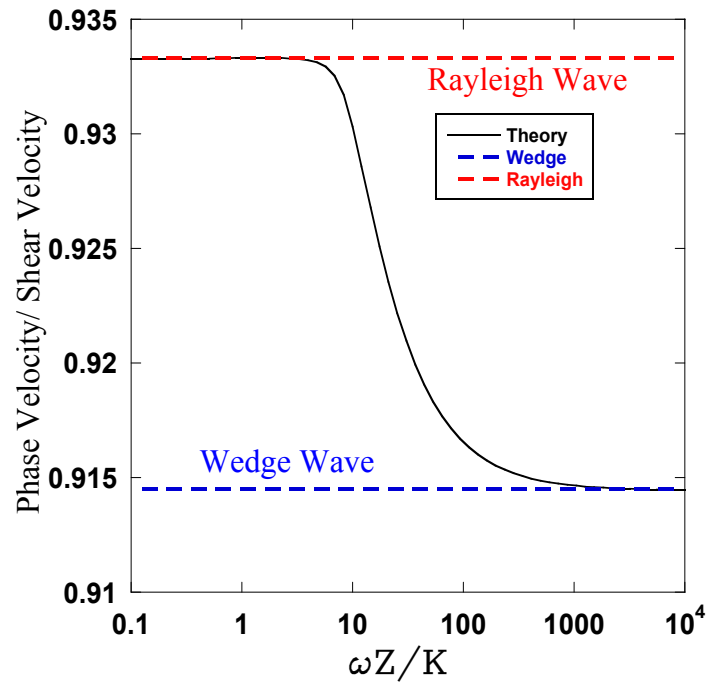
FIG. 2. *Normalized phase velocity vs. normalized stiffness. ω is the frequency, Z is the impedance ρv_{shear} and κ is the stiffness. The above result is from several stiffness and frequency sweeps. Note that at low stiffness the theory predicts a wedge wave velocity and at high stiffness the Rayleigh velocity is predicted*

FIG. 3. *Aluminum samples inside the Instron 100 klbs load frame. The bottom two blocks form the geometry of Figure 1, and the top block is used as a spacer to help distribute load evenly along the surface. The transducer frame can be seen holding the array platen on the left side of the blocks.*
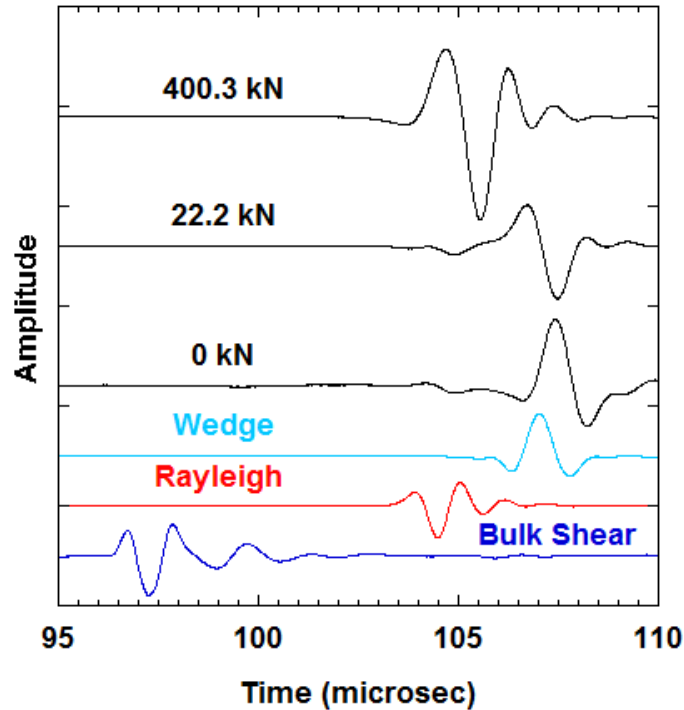
FIG. 4. *Seismic waveforms for the bulk, Rayleigh, wedge, and RW waves. The RW wave is stress dependent and is shown for 0 kN, 22.2 kN and 400.3 kN loads. Note that as the load increases, the RW wave converts from the wedge to the Rayleigh wave velocity.*

characterized for a given applied stress.

The source transducers were excited using a square-wave pulse of 400V with a repetition rate of 1000 Hz from an Olympus 5077PR pulse generator. These signals were received and recorded in a National Instruments PXI-1042 controller with a PXI-5122 digitizer and then stored for analysis.

2.7. Polarization. S-wave transducers were used to propagate waveforms along the coupled wedge at several polarizations. Previous research by DeBilly et al. [17] found that the polarization of the shear wave propagating along single wedges played a vital role in the amplitude of the received signal.

Using the angle, θ, defined in Figure 1, it was determined that the polarizations with the highest amplitude was at $0°$ relative to the fracture plane. This was in agreement with the displacement amplitudes calculated from the numerical section of the paper.

3. Results. The waveforms recorded through the bulk, along the surface and along the fracture were found to be in agreement with previous experimental and theoretical work on interface waves [5-12] and Rayleigh waves [25]. The mode observed along the intersection of the two blocks was not in agreement with any previously discussed results nor previously observed. Waveforms at each load were analyzed and found to be in agreement with the theoretical formulation discussed above. When no load was applied to the fracture, the observed RW waveform matched the wedge wave observed for either block, i.e., essentially a contact with zero stiffness. As the load was increased, and the fracture closed, the signal was observed to increase in velocity such that at high loads (> 100 kN) the fracture had closed and the velocity matched that of the Rayleigh wave (Figure 4).

This observed RW waveform is the first evidence that the guided mode from wedge waves, which couples through the points of contact along the surface expression of a fracture, exists, is dispersive and depends on the stiffness of contact.
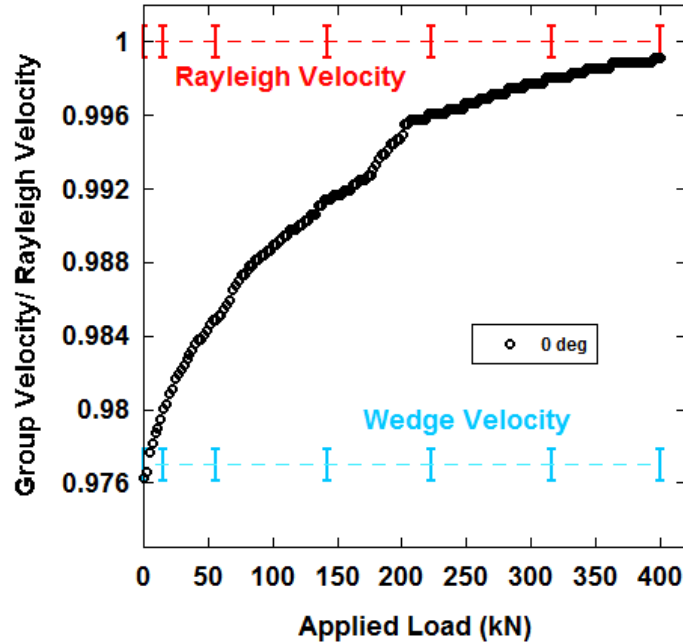
FIG. 5. *Experimental group velocity, normalized by Rayleigh velocity, as a function of applied load from the load frame. Group velocities were calculated from the wavelets for $0°$ using a frequency of 0.4 MHz. Error bars are shown for the wedge and Rayleigh velocity from experimental measurements on both blocks of aluminum. Error bars for the data fall within the size of the symbols.*

3.1. Wavelet Analysis. A Morlet wavelet [26] of the recorded seismic waveform was performed for all of the applied loads to calculate the group velocity. A wavelet transform, that calculates the energy density of the waveform as a function of time and frequency simultaneously, indicated that the peak in the energy spectrum occurred around 0.4 MHz for this sample geometry and 0.65MHz for the intact sample.

The group velocities were then calculated from each wavelet using the arrival time of the dominant energy for 0.4 MHz and are shown as a function of applied load in Figure 5. Using the normalized dispersion curve (Figure 2), an estimate of the stiffness at the fracture edge was obtained.

4. Discussion. The experimental results show that a coupled wedge mode, known as a Rayleigh Wedge mode, does indeed exist at the surface of a material along a fracture and is in the theoretically derived range of velocities. First order assumptions for displacement discontinuities resulted in very accurate theoretical velocities compared to those observed in the experiment.

The experimental and theoretical results show that coupled-wedge modes do exist even when medium 1 and medium 2 have the same material properties. Unlike the RS wave, which is also a guided coupled mode, there are no restrictions on whether the media must be the same or different, thus a similar guided-mode should also exist when the media are different and in partial contact.

This study has given rise to a new and powerful tool for estimating fracture stiffness along coupled quarter planes. This technique can be used in conjunction with the well established interface wave characterization in seismically measuring the fracture stiffness and how it varies with depth along a fracture.

This new technique has opened up a new set of topographic features which can be explored for both geophysical and engineering applications such as structural integrity, dike structures, outcrops, and other intrusions found on different geologies on earth [27, 28]. It has also given field work another tool to help in the correct interpretation of seismic data to prevent common misconceptions from

shallow seismic analysis [29].

5. Conclusion. The theoretical derivation described here hypothesized the existence of a new type of guided waveform for a geometry with two elastic quarter planes in contact along their edge. Using a coupled wedge wave approach with a Laguerre polynomial expansion and displacement discontinuity boundary conditions a characteristic determinant was derived (Equation 10). The RW-mode was found to propagate with a velocity that is a function of both frequency and stiffness. By normalizing the theoretical results (Figure 2), the theory can be scaled to frequencies used in the field to determine the range of fracture stiffnesses that can be detected for a given frequency. Future work in this area should include experimental verification of the effect of different media, a parameter study of the range of existence for this coupled wedge mode and theoretical work on four wedges coupled to form a fracture intersection. Rayeligh-Wedge waves provide an additional characterization tool for monitoring the alteration of surface fractures caused by stress.

REFERENCES

[1] Lin, S., Ashlock, C., "A study on Issues Relating to Testing of Soils and Pavements by Surface Wave Methods", AIP Conf. Proc., **1430**, 1532–1539, (2012)

[2] Wang, L., Luo, Y. and Xu, Y., "Numerical Investigation of Rayleigh-wave Propagation on Topography Surface", J. Appl. Geophysics, **86**, 88-97, (2012)

[3] Xia, J., Miller, R. D. and Park, C. B., "Estimation of Near-Surface Shear-Wave Velocity by Inversion of Rayleigh Waves", Geophysics, **64**, 691-700, (1999)

[4] Murty, G.S., "Theoretical Model for Attenuation and Dispersion of Stoneley Waves at Loosely Bonded Interface of Elastic Half Spaces, Physics of the Earth and Planetary Interiors, 11, 65-79, (1975)

[5] L. J. Pyrak-Nolte, N. G. W. Cook, "Elastic Interface Waves Along a Fracture", Geophysical Research Letters, **14**, 1107-1110, (1987)

[6] Gu, B.L., "Interface Waves on a Fracture in Rock, University of California, Berkeley, PhD. Thesis. , (1994)

[7] Pyrak-Nolte, L., Cook, N. G. W., and Myer, L. R., "Seismic visibility of Fractures, Rock Mechanics: Proceedings of the 28th US Symposium, (1987)

[8] Gu, B.L., Nihei, K.T., Myer, L.R. and Pyrak-Nolte, L. J., "Fracture Interface Waves, Journal of Geophysical Research-Solid Earth, 101, 827-835, (1996)

[9] Pyrak-Nolte, L. J., Myer, L. R. and Cook, N. G. W., "Transmission of Seismic Waves Across Single Natural Fractures", J. of Geophysical Res., 95, 8617-8638, (1990)

[10] Pyrak-Nolte, L. J., Myer, L. R. and Cook, N. G. W., "Anisotropy in Seismic Velocities and Amplitudes from Multiple Parallel Fractures", J. of Geophysical Res., 95, 11,345-11,358,(1990)

[11] Pyrak-Nolte, L.J., Xu, J.P. and Haley, G.M., "Elastic Interface Waves Propagating in a Fracture, Physical Review Letter, 68, 3650-3653, (1992)

[12] Pyrak-Nolte, L.J., Xu, J.P. and Haley, G.M, "Elastic Interface Waves along a Fracture- Theory and Experiment, Proceedings of the 33rd US Symposium, 999-1007, (1992)

[13] M. Schoenberg, "Elastic Wave Behavior Across Linear Slip Interfaces", J. Acoust. Soc. Am, **68**, 1516–1521, (1980)

[14] Abell, B. C., Pyrak-Nolte, L.J., "Shear Specific Stiffness of Fractures and Fracture Intersections, Proceedings of the 46th US Symposium, No. 12-294, (2012)

[15] P.E. Lagasse, "Analysis of a Dispersionfree Guide for Elastic Waves", Electronics Letters, **8**, 372 – 373, (1972)

[16] A. Maradudin, R.F. Wallis, A.A. Mills, and R. L. Ballard, "Vibrational Edge Modes in Finite Crystals," Physical Review B, **6**, 1106–1111, (1973)

[17] M. DeBilly, "Acoustic Technique Applied to the Measurement of the Free Edge Wave Velocity", Ultrasonics, **34**, 611-619, (1996)

[18] E. Sokolova, A. Kovalev, A. Maznev and A. Mayer, "Acoustic Waves Guided by the Intersection of a Surface and an Interface of Two Elastic Media", Wave Motion, **49**, 388–393, (2012).

[19] A. Maradudin,"Edge Modes," Japan J. Appl. Phys. Suppl., 2 **2**, 871–878, (1974)

[20] D. B. Bogy, "Two Edge-Bonded Elastic Wedges of Different Materials and Wedge Angles Under Surface Tractions", Journal of Applied Mechanics, 377–386 ,(1971)

[21] Kitsunezaki, C., "Behavior of Plane Waves Across a Plane Crack, J. Mining Coll. Akita Univ., Series A , 6 (3), 173-187, (1983)

[22] C. Hobday, M. H. Worthington, "Field Measurements of NOrmal and Shear Fracture Compliance", Geophysical Prospecting, **60**, 488–499, (2012)

[23] R. Lubbe, J. Sothcott, M. H. Worthington and C. McCann, "Laboratory Estimates of Normal and Shear Fracture Compliance", Geophysical Prospecting, **56**, 239–247, (2008)

[24] Choi, M. K., Pyrak-Nolte, L. J. and Bobet, A., "Relationship between Shear and Normal Stiffness in a Fracture Subjected to Mixed-Mode Loading, 47th US Rock Mechanics/ Geomechanics Symposium, San Francisco, 13-405, (2013)

[25] Lord Rayleigh, "On Waves Propagated along the Plane Surface of an Elastic Solid", Proc. R. Soc. Lond. A, **17**, 4-11, (1885)

[26] L. J. Pyrak-Nolte, D. D. Nolte, "Wavelet Analysis of Velocity Dispersion of Elastic Interface Waves Propagating along a Fracture", Geophysical Research Letters, **22**, 1329-1332, (1995)

[27] Niederleithinger, E., Weller, A. and Lewis, R., "Evaluation of Geophysical Techniques for Dike Inspection", JEEG, 17, 185-195, (2012)

[28] Hall, S. A, Lewis, H. and Macle, X., "Improved Seismic Identification of Inter-fault Damage Via a Linked Geomechanics-seismic Approach", Geological Society, London, Special Publications 2007, 289, 187-207; doi:10.1144/SP289.11, (2007)

[29] Ismail, A., Smith, E., Phillips, A. and Stumpf, A., "Pitfalls in Interpretation of Shallow Seismic Data, Applied Geophysics, 9, 87-94; doi:10.1007/s11770-012-0318-4, (2012)